

Biochar applications and modern techniques for characterization

Farrukh Raza Amin^{1,2} · Yan Huang² · Yanfeng He² · Ruihong Zhang³ ·
Guangqing Liu² · Chang Chen^{1,2,4}

Received: 19 March 2016 / Accepted: 18 May 2016 / Published online: 22 June 2016
© Springer-Verlag Berlin Heidelberg 2016

Abstract Biochar simply is the material produced when biomass undergoes any chemical processes under the conditions of pyrolysis. The variety of biomasses, including wood waste, agricultural crop leftover, organic waste, animal manure, and forestry residues, have been considered as raw material to produce biochar. Biochar is widely used for generation of heat and power and an addition to soils, in which it serves as a fertilizer and carbon sequestration agent. Also in the form of being activated, it finds significant role for various adsorption applications. The most beneficial use of a given char depends on its physical and chemical characteristics, even though the relationship of char properties to these applications is not well defined. Various widely used modern analytical techniques, which are applicable and crucial for biochar characterization, have been reviewed in the present work, such as solid state nuclear magnetic resonance spectroscopy, Fourier transform infrared spectroscopy, scanning electron microscopy, transmission electron microscopy, X-rays photoelectron spectroscopy, X-rays diffraction, thermogravimetric analysis, near edge X-rays absorption fine structure

spectroscopy, and gas chromatography-mass spectroscopy. Utilization of these modern techniques provides the quantitative as well as qualitative information, i.e., determining the sizes, shapes, and physicochemical characteristics of biochar, which is reliable to track changes in the carbon arrangement over reaction time and temperature, and will be useful for efficient production of biochar and application. It provides the useful information for the researchers in this area and is beneficial not only for the effective biochar production, but also for potential utilization/application, and not only for environment but also for agriculture.

Keywords Analytical techniques · Application · Biochar · Biomass · Characteristics · Production

List of abbreviations

Ag	Silver
As	Arsenic
BPB	Birnessite-modified pine biochar
C	Carbon
Cd	Cadmium
Co	Cobalt
CO ₂	Carbon dioxide
CP	Cross polarization
Cr ⁶⁺	Chromium VI
CT	Computerized tomography
Cu	Copper
DAWC	Digested dairy waste biochar
DP	Direct polarization
DSTC	Digested sugar beet tailing biochar
DWSBC	Digested whole sugar beet biochar
FTIRS	Fourier transform infrared spectroscopy
GC-MS	Gas chromatography-mass spectroscopy
H	Hydrogen

✉ Chang Chen
chenchang@mail.buct.edu.cn

¹ College of Life Science and Technology, Beijing University of Chemical Technology, Beijing 100029, China

² Biomass Energy and Environmental Engineering Research Center, College of Chemical Engineering, Beijing University of Chemical Technology, Beijing 100029, China

³ Department of Biological and Agricultural Engineering, University of California, Davis, CA 95616, USA

⁴ Present Address: 505 Zonghe Building, Beijing University of Chemical Technology, 15 North 3rd Ring East Road, Beijing 100029, China

K	Potassium
MgEC	Magnesium enrich biochar
MPB	Manganese oxide-modified pine biochar
N	Nitrogen
NEXAFS	Near edge X-rays absorption fine structure spectroscopy
Ni	Nickle
NMRS	Nuclear magnetic resonance spectroscopy
NO ₃ ⁻	Nitrates
O	Oxygen
P	Phosphorus
PAHs	Poly-aromatic hydrocarbons
Pb	Lead
SAXS	Small angle X-rays scattering
Sb	Antimony
SEM	Scanning electron microscopy
TEM	Transmission electron microscopy
TGA	Thermogravimetric analysis
VM	Volatile matter
XPS	X-rays photoelectron spectroscopy
XRD	X-rays diffraction
Zn	Zinc
ZVI	Zerovalent iron

Introduction

The biochar is originally found from the ancient Amerindian inhabitants in the Amazon region, commonly termed as Terra Preta de Indio, where dark earth was formed using char and slash techniques (Lehmann and Joseph 2009). Biochar is yielded from the pyrolysis of biomass such as wood and grass, with the limited supply of nitrogen (N) or oxygen under intense heat conditions (Rutigliano et al. 2014). In recent years, a number of academic papers has been published, based on the exploitation of biological carbon assessments, we may get the impression that, in environmental management, as well as in agriculture, a new era has begun (Vochozka et al. 2016a). Various raw materials for biochar production may be subjected to the pyrolysis process, and as per findings from the literature, the physicochemical properties of the biochar vary from one raw material to another. Biochar properties are highly influenced by the temperature at which pyrolysis occurs. The extent of carbonization of the raw material increases with increasing pyrolysis temperature, as indicated by increased carbon (C) content also decreased hydrogen (H) and oxygen contents in the resulting biochar. Biochar is characterized with its lower specific surface area, higher water-holding capacity, lower pH, more -COOH and C₆H₅OH groups, and higher cation exchange capacity (CEC), when pyrolysis happens at low temperature (Ippolito et al. 2012).

The authors classified a diversity of physical and chemical properties of biochar for production and application, as predominantly controlled by either feedstock or temperature. While this preliminary knowledge is critical to guide the production of designing biochar, it falls short when the influence of both parameters is significant, as in the case with most properties of interest (Zhao et al. 2014; Morales et al. 2015). In this review, the factors affecting the biochar production such as pyrolysis conditions (retention time, feedstock types, temperature, and heat transfer rate), and consequently its applications for contaminant remediation are debated in detail. Special prominence is given to the mechanistic evidence of the interaction of biochar with soil and water contaminants. Therefore, this review is limited to apply biochar as a green environmental sorbent for the soil and water polluted with organic and inorganic pollutants. Identification of biochar through modern analytical techniques is likely to result in variations in its surface properties such as surface area, surface charge, functional groups, and pore volume and distribution. Applicability and performance of biochar depend upon the type of contaminants (i.e., polar/non-polar, anionic/cationic, hydrophilic/hydrophobic, and inorganic/organic), environmental conditions, remediation goals, and land use purpose in general. Although a lot of focus is given to the characterization of biochar, but still practically this has been lacking in some aspects as researchers might be provided with limited facilities such as resources and instrumentations. The main objective of characterization is to differentiate biochar from soil organic matter and other forms of black carbons yielded from varieties of biomasses. Some of the modern techniques (ssNMR, FTIR, XRD, XPS, SEM, TEM, TGA-DTG, GC-MS, and NEXAFS) that most effectively differentiate various types of biochar can also be used to characterize individual biochar wastes (or collection of fragments) recovered from both soil and solution systems. The utilization of these methods depends on specific analysis and the final target to achieve (Lou et al. 2012). For optimization and proper selection, the efforts to compare all available modern analytical techniques, therefore, are needed, thereby directing the interpretation of differently obtained data and proposing appropriate modern techniques for analysis. In the present work, a set of different modern analytical techniques is reviewed which resulted as valuable information in a comparative way to determine their analytical characterization of biochar.

Biochar benefits

The major utilization of biochar is found in four major areas, where biochar is being used in environmental management include (1) soil improvement, (2) waste

management, (3) climate change mitigation, and (4) energy generation (Ahmad et al. 2014; Zhou et al. 2014a; Turrado Fernández et al. 2015). Among these four areas, we have focused on soil improvement in our study. In comparison to stability, agronomic application of biochars has not been an absolute value, as it requires to match local soil constraints. The biochar influence on chemical properties of acidic soil is steady with their chemical configuration and application of alkali biochar significantly rises the sorption of phosphorus (P) and decreases the obtainability of adsorbed phosphorus. Biochar's effects on soil P are related to their chemical properties and surface properties (Chintala et al. 2013, 2014). Raw materials, which are woody in nature, show the highest relaxation with range of pH value from 4 to 9 (Enders et al. 2012). The quantity of acidic functional groups exist on biochar surface is 10 times greater than others, ultimately their CEC is high (Beesley et al. 2011; Mukherjee et al. 2011). Recent investigations reveal that the biochars will have better use to increase soil CEC at lower temperature or on the other hand biochars will become alkaline and reduce the yield of biochar (Hossain et al. 2011).

Biochar, the product of different biomasses can provide an alternative sources of long-term C storage in soil to minimize climate variation by an enhancement in the biogenic C collection, decrease greenhouse gas emissions (Ubando et al. 2014), restore soil fertility (Novak and Busscher 2013), amend soil physical properties such as pH, pore structure, surface area, and mineral matter (Jaafar et al. 2014), enhance crop yield and productivity (Chintala et al. 2014; Lashari et al. 2014), and reduce N emission and leaching (Spokas et al. 2012). Examples of the specific biochar properties accounted for these benefits are summarized in Table 1.

Biochar production and properties

Biomass pyrolysis

For the sustainable biochar production, biomass assets may be limited. Such as biomasses attained from agricultural sources may clue to an increase in erosion and decline in soil fertility (Cowie et al. 2012). Mainly feedstocks are divided into two groups: (1) predominantly yielded biomass being energy and biochar source, and (2) biomass waste as a byproduct. Waste biomass finds wide range of applications regarding the biochar production due to its reasonable cost and food security benefits related to other types of biomass (Ahmad et al. 2014).

Kinetics of biomass pyrolysis process plays a vital role in research. The three components of the material (lignin, cellulose, and hemicellulose) are initially optimized

according to the possible mixture design scheme. After that, the fast pyrolysis of three components and their mixtures are examined in a TGA to explore the pyrolysis characteristics of the mixtures and synergistic association among the three components (Zhang et al. 2016). Using chemical decomposition of biomass at temperature ranging from 200 to 900 °C in the existence of minute oxygen, biochar can be produced and is generally known as pyrolysis. The rate of pyrolysis process is commonly associated with the retention time and operating temperature as shown in Table 2. Fast pyrolysis process with a very small retention time (<2 s) is mostly applied to yield bio-oil from biomass giving about 75 % bio-oil. Slow and moderate pyrolysis processes with a retention time from the few minutes to many hours or even days are usually preferred for biochar yield up to 35 % (Ahmad et al. 2014). Gasification is altered by a common pyrolysis process. It involves the conversion of biomass into gases which is known as syngas enriched with H and carbon monoxide (CO), and this change occurs at the high temperature, which may be >700 °C with a controlled supply of oxygen (Mohan et al. 2007).

Physical and chemical properties of biochar

The variations in the physical properties of the biochars are obvious and can be easily observed with visualization, particularly when these are in a loose, granular, or pelleted form. Usually, the fined biochars are melted easily and rapidly than pelleted. These changes will affect the ability of biochar mixing into soils, also some significant physical parameters such as specific surface area surface charge, particle size distribution, porosity, bulk density and specific gravity, water-holding capacity, and hydraulic conductivity (Zimmerman 2010). Uniform mixing of biochar pellets may be largely difficult than modifying soil with a better quality biochar. Biochars with high ash content have smaller life span in natural soil system because of higher rates of degradation (Huisman et al. 2012).

Commonly, biochars prepared in the pyrolysis process showed a variety of chemical properties such as pH measurement, elemental analysis, CEC analysis, and zeta potential of biochar colloids through different methods (Nartey and Zhao 2014). As perceived in previous studies, the fast pyrolysis biochars not only have finer structure due to rapid change in a fast pyrolysis reactor, but also hold a higher grade of thermal modification as indicated by its low H and C ratio than the slow pyrolysis or gasification biochars (Yargicoglu et al. 2015). Rest of the properties, such as determined pH (Brewer et al. 2014) and surface area (Cheng and Lehmann 2009), are also in association with rapid rate of carbonization, steady with observations in prior biochar characterization studies (Bruun et al. 2011).

Table 1 Biochar benefits

Biochar components	Soil and environmental benefits	References
Soil salinity	Biochar can improve salt stress effects on plants and to mitigate salinity in agricultural soils	(Lashari et al. 2014)
Ca, K, Mg, Na, Fe, Mn, Zn [Total (mg kg ⁻¹)]	Micronutrients can increase the soil fertility through biochar addition	(Chintala et al. 2013; Morales et al. 2015)
Yield (%)	During the pyrolysis process the production amount of biochar is dependent on yield	(Morales et al. 2015)
Carbon (mg g ⁻¹)	Amount of total C in organic matter benefits the soil	(Morales et al. 2015)
pH _w (-)	Determination and attraction of nutrients and mineral ions directly affect the soil surface charge due to the pH of the soil solution	(Chintala et al. 2014)
Microbial habitat	Soil microbial biomass, activity, and the degree of response appear to be dependent on nutrient availability increases in soil due to biochar	(Jaafar et al. 2014)
Bulk density (Mg m ³)	The density of compacted soil reduced using of low-bulk density biochar	(Novak and Busscher 2013)
Volatile matter (%)	Biochar long life in the soil affects by the VM because residuals volatiles impact on organic substance sorption by obstructing pores and varying surface chemical interactions	(Novak and Busscher 2013)
GHG emissions	Biochar reduces N ₂ O and CH ₄ emissions from agriculture sectors, and can be locked in soil as C storage	(Feng et al. 2012)
P, S [Total (mg kg ⁻¹)]	Biochar can improve the soil fertility by adding the macronutrients	(Spokas et al. 2012)
Nitrogen (mg g ⁻¹)	Total nitrogen works as macronutrients in the biochar supply. For nitrogen rich soil amendment, biochar may strongly sorb ammonia	(Dempster et al. 2012; Razon 2014)
Fixed carbon (%)	Non-labile fixed carbon is a property butted to biochar stability	(Enders et al. 2012; Rajkovich et al. 2012)
Specific surface area (N ₂), (CO ₂) (m ² g ⁻¹)	SSA of the high nano/micro-pore may increase the sorptive property of organic compounds to biochars and increase water-holding capacity of soil	(Beesley et al. 2011; Karhu et al. 2011)
Electric conductivity (EC) (mS m ⁻¹)	EC shows the quantity of salt enclosed in the biochar. Soil structure can stabilize on high EC	(Hossain et al. 2011)
Ash (%)	Sorption ability of biochar for organic/inorganic compounds increases by the increase of ash percentage	(Cao et al. 2011)
Carbon nitrogen ratio (-)	Rate of decomposition of organic matter and release of soil nitrogen is affected by C:N	(Novak et al. 2009)
Poly-aromatic hydrocarbons (PAHs)	Biochar improves soil sorption capacity of PAHs, pesticides and herbicides, and therefore influence toxicity, transport and fate of such contaminants	(Hiller et al. 2008)
Cation exchange capacity [Av (mmol _c kg ⁻¹)]	The soil's ability to hold and exchange cations can be improved by an increase of CEC	(Glaser et al. 2002)

Factors affecting biochar properties

During the pyrolysis process, reaction conditions play a very important role for the production of biochar. Biochar properties are influenced by the process parameters such as particle size, processing time, heating rate, temperature, and many more. These operating parameters not only affect the quality of the pyrolysis products but also control its yield (Tripathi et al. 2016). The significant key parameters considered in recently published studies on biochar production and their properties are summarized in Table 2. A number of feedstocks as well as crop residues, wood biomass, animal litter, and solid wastes have been utilized to produce biochar via slow to fast pyrolysis processes. The pyrolysis temperature in these studies varied from 100 to 1000 °C with a processing temperature ranging

from 3 to 20 °C min⁻¹. Biochar yield is strongly feedstock, pyrolysis, and processing temperature dependent. Usually, animal litter and solid wastes produce a high yield of biochar related to that from crop residues and wood biomass (Enders et al. 2012; Alper et al. 2014).

The huge production is related to the larger inorganic contents of the feedstock materials, as specified by their relatively high ash contents, proposed that various inherent metals in animal litter may protect against the loss of volatile material by varying the energy required for bond dissociation of organic and inorganic C bonds. Usually, biomass with high lignin content results in higher biochar yield (Cantrell et al. 2012).

Operating temperature is the least effective factor in determining biochar yield. Raising the operating temperature with a range of 3–20 °C min⁻¹ would slightly

Table 2 Production of biochar by different sources and their operating conditions

Biochar sources	Moisture contents (%)	Pyrolysis unit	Grain size (µm)	Biomass quantity	Processing temperature	Oxygen limitations	Retention time (min)	Pyrolysis temp. (°C)			References
								Low	Moderate	High	
<i>Quercus rotundifolia</i> (Oak)	n/a	Horizontal tube furnace	177–250	n/a	Continuous flow	N ₂	120	300	450	600	(Morales et al. 2015)
Rapeseed	12.6	Tubular reactor	<1000	30 g	3 °C 15–20 min ⁻¹	N ₂	30	400	500	600	(Morales et al. 2015)
Aged oak and hickory wood	66.2	Missouri type concrete kiln	4750	10 g	Continuous flow	n/a	n/a	–	500	–	(Brewer et al. 2014; Yargicoglu et al. 2015)
Bull Manure	10	Kiln	149–850	3 kg	3 °C 15–20 min ⁻¹	N ₂	90	300	450	600	(Enders et al. 2012)
Corn	10	Kiln	149–850	3 kg	3 °C 15–20 min ⁻¹	N ₂	90	300	450	600	(Rajkovich et al. 2012)
Dairy Manure	10	Kiln	149–850	3 kg	3 °C 15–20 min ⁻¹	N ₂	90	300	450	600	(Enders et al. 2012)
Digested dairy Manure	10	Kiln	149–850	3 kg	3 °C 15–20 min ⁻¹	N ₂	90	300	450	600	(Enders et al. 2012; Rajkovich et al. 2012)
Food Waste	10	Kiln	149–850	3 kg	3 °C 15–20 min ⁻¹	N ₂	90	300	350	600	(Rajkovich et al. 2012)
Oak	10	Kiln	149–850	3 kg	3 °C 15–20 min ⁻¹	N ₂	90	300	450	600	(Enders et al. 2012; Rajkovich et al. 2012)
Paper waste	10	Kiln	149–850	3 kg	3 °C 15–20 min ⁻¹	N ₂	90	300	425	600	(Vochozka et al. 2016b)
Pine	10	Kiln	149–850	3 kg	3 °C 15–20 min ⁻¹	N ₂	90	300	450	600	(Enders et al. 2012; Rajkovich et al. 2012)
Poultry litter	10	Kiln	149–850	3 kg	3 °C 15–20 min ⁻¹	N ₂	90	300	450	600	(Enders et al. 2012; Rajkovich et al. 2012)
Hazelnut	10	Kiln	149–850	3 kg	3 °C 15–20 min ⁻¹	N ₂	90	300	450	600	(Enders et al. 2012; Rajkovich et al. 2012)
Canola straw	n/a	Batch pyrolysis	n/a	n/a	20 °C	n/a	20	400	750	1000	(Tong et al. 2011)
<i>Pinus taeda</i> (Pine)	5d drying at 60 °C	Batch pyrolysis oven	50,000	4749 cm ³	26 °C	N ₂	60	250	400	650	(Mukherjee et al. 2011)
<i>Tripsacum floridanum</i> (Grass)	5d drying at 60 °C	Batch pyrolysis	50,000	4749 cm ³	26 °C	N ₂	60	250	400	650	(Mukherjee et al. 2011)
<i>Quercus lobata</i> (Oak)	5d drying at 60 °C	Pyrolysis oven	50,000	4749 cm ³	26 °C	N ₂	60	250	400	650	(Mukherjee et al. 2011)
<i>Pinus ponderosa</i> (Pine)	n/a	Muffle furnace	<1500	n/a	n/a	Yes	60	300	425	600	(Keilueit et al. 2010)
<i>Tall fescue</i> (Grass)	n/a	Muffle furnace	<1500	n/a	n/a	Yes	60	300	350	600	(Keilueit et al. 2010)
<i>Pinus taeda</i> (Pine)	n/a	Batch pyrolysis unit	n/a	n/a	n/a	N ₂	n/a	400	450	500	(Gaskin et al. 2008)
Poultry litter	n/a	Batch pyrolysis unit	n/a	n/a	n/a	N ₂	n/a	400	450	500	(Gaskin et al. 2008)
<i>Pinus halepensis</i> (Pine)	n/a	Horizontal tube furnace	177–250	n/a	Continuous flow	N ₂	120	300	450	600	(Cordero et al. 2001)

n/a not applicable

decrease in biochar yield. At the similar temperature, a prominent increase in aromatic C and the appearance of condensation reactions are observed by the near edge X-ray absorption fine structure spectra of the biochars (Keiluweit et al. 2010). Elemental analysis and their calculated molar ratios have been widely used in conjunction with Fourier transform infrared spectroscopy to reveal the pyrolysis temperature influences on the functional chemistry of biochars (Lian et al. 2011).

The pyrolysis temperature influences on the morphology and surface structural changes in biochar (Uchimiyu et al. 2011b). Commonly, surface area is found to increase with high temperature. However, a drop in surface area at 700 °C has also been investigated. A positive correlation between micro-pore volume and surface area proposes that the pore size distribution serves to be very important factor to increase the surface area in biochar. Biochars produced from animal litter and solid waste feedstocks exhibit lower surface areas compared to biochars produced from crop residue and wood biomass, even at higher pyrolysis temperatures. Notably, the biochars produced at 700 °C and a lower heating rate may possess a lower surface area. This lowering in surface area may be due to the development of deformation, cracking, or blockage of micro-pores in biochars (Lian et al. 2011).

However, poultry manure and sewage sludge resulting biochars do not undergo de-polymerization because of the absence of lignocellulosic compounds. Generally, no significant effect of pyrolysis temperature on Nitrogen contents of biochars derived from various feedstock was observed. While, it depends on the type of feedstock. Manure and sewage sludge-based biochars are generally N enriched, relative to other elements. A little information is available on sulfur and phosphorus contents of biochar that can further add complexity to S and P cycles in soil. In addition, functional groups with oxygen and sulfur contents enhance ammonia retention on char by forming ammonium sulfate salts. Therefore, the role of functional groups in biochar should be addressed for better understanding of biochar effects on nutrient cycling in soil (Petit et al. 2010).

Generalized analytical techniques for biochar analysis

Clearly, it has been seen that structural analysis of biochar will influence its flexibility in the environment and its interactive function with the soil hydrologic cycle and appropriateness of being a biological role for soil microorganisms. However, the broad range of biochar structural characterization caused it challenging to study methods and appropriate to connect the fundamental

physical properties of density and porosity to environmental benefits.

Since the long period, carbonaceous materials have been regarded as adsorbents of various contaminants in water and soil either organic or inorganic in nature (Ahmad et al. 2012; Yang et al. 2013). Biochar has similarities with activated carbon in many aspects such as mutual production during pyrolysis and medium to large surface areas (Cao et al. 2011). Also, the biochar surrounds a non-carbonized fraction that may undergo change with soil impurities. Specially, the level of oxygen containing carboxyl, hydroxyl, and phenolic surface functional groups in biochar could efficiently hold together the soil contaminants (Uchimiyu et al. 2011a). The interaction of different metals with biochars is a complex function of pH such as (1) the biochar functions vary with pH and (2) the metals pollutant ion speciation changes with pH that leads to a far more complex situation than either alone. These sorts of biochar characteristics revealed the potential of being highly active adsorbent for most of the impurities in soil and water as shown in Table 3. As discussed previously, the biochar properties are mainly affected by temperature, retention time, and feedstock type, which strongly impacts biochar sorption properties toward various pollutants/impurities. Therefore, the selection of proper biochars yielded at different operating conditions should be given proper consideration (Maroušek 2014).

In the present work, the use of elemental analysis, structural, and functional group properties measurement techniques are reported to characterize biochar. These all techniques are used to estimate the relationship between biochar's physical properties and its behavior toward the environment (Brewer et al. 2014). Nowadays a huge variety of modern techniques have been utilized, including elemental analysis and molecular indicators. These techniques are solid state nuclear magnetic resonance (ssNMR) spectroscopy, X-rays diffraction (XRD), near edge X-rays absorption fine structure spectroscopy (NEXAFS), X-rays photoelectron spectroscopy (XPS), transmission electron microscopy (TEM), scanning electron microscopy (SEM), thermogravimetric and derivative thermogravimetric analysis (TGA-DTG), Fourier transform infrared spectroscopy (ATR-FTIR), and gas chromatography–mass spectrometry (GC–MS) (McBeath et al. 2011; Charon et al. 2014). In the following section, all analytical techniques widely applied for determining biochar characterization are discussed in detail.

Solid state nuclear magnetic resonance (ssNMR) spectroscopy

Solid state ^{13}C NMR spectroscopy is used to estimate the carbon chemistry of biochars generated from different

Table 3 Summary of various biochar sorbents and techniques

Biochar sorbents	Target substances	Analytical techniques									Matrix	Peak temp. (°C)	References	
		ssNMR	FTIR	SEM	XRD	TGA-DTG	TEM	NEXAFS	XPS	GC-MS				
Woody feedstock biochar (Pine, grass species, and citrus)	As and Pb					✓						Soil	400	(Wang et al. 2015a)
Soybean stover-derived biochar	Sb		✓									Water	500	(Vithanage et al. 2015)
Wheat straw biochar	PAHs										✓	Water	400	(Chen et al. 2015)
Iron-impregnated biochar (hickory)	As		✓	✓	✓	✓				✓		Water	600	(Hu et al. 2015)
MPB and BPB	As and Pb			✓	✓						✓	Water	600	(Wang et al. 2014)
Magnetic biochar (natural hematite, pinewood)	Pb			✓	✓	✓				✓		Water	600	(Wang et al. 2015b)
Biochar (chestnut, pinewood, fescue)	C	✓							✓			Soil	350–600	(McBeath et al. 2014; Wiedemeier et al. 2015)
Magnetic and nonmagnetic energy cane biochar	Pb		✓	✓	✓		✓					Water	450/fast pyrolysis	(Mohan et al. 2015)
ZVI biochar	As, Pb, Ag and Cr ⁶⁺			✓	✓	✓						Water	600	(Zhou et al. 2014a; Zhou et al. 2014b)
Sugarcane bagasse, hickory wood biochar	CO ₂		✓			✓						Soil	300 450 600	(Creamer et al. 2014)
Clay biochar carbon composite	Pb			✓	✓	✓						Water	600	(Yao et al. 2014)
Sugarcane bagasse biochar	Pb		✓									Water	250–600	(Ding et al. 2014)
Magnetic oak wood and bark biochar	Pb, Cd		✓	✓	✓	✓	✓					Water	450	(Mohan et al. 2014a)
MgEC	P			✓	✓	✓						Water	600	(Yao et al. 2013)
Biochar/MgAl-LDH (composite)	P		✓	✓	✓							Water	600	(Zhang et al. 2013b)
Biochar/γ-Fe ₂ O ₃ (composite)	As			✓	✓		✓			✓		Water	600	(Zhang et al. 2013a)
Biochar/AlOOH nanocomposite	As			✓	✓		✓					Water	600	(Zhang and Gao 2013)
Sewage sludge biochar	As, Cd, Cr, Co, Cu, Ni, Pb, Zn and PAHs			✓	✓							Soil	500–550	(Khan et al. 2013; Khan et al. 2014)
Soil amended PAHs biochar (reference biochar)	PAHs									✓		Soil	300	(Fabbri et al. 2013)
DAWC and DWSBC	K, Pb, Cu, Ni and P		✓	✓	✓							Water	600	(Inyang et al. 2012)

Table 3 continued

Biochar sorbents	Target substances	Analytical techniques								Matrix	Peak temp. (°C)	References	
		ssNMR	FTIR	SEM	XRD	TGA-DTG	TEM	NEXAFS	XPS				GC-MS
MgO-Biochar nanocomposite	P, Nitrates			✓	✓	✓	✓				Soil	600	(Zhang et al. 2012a)
Turkey litter biochar	K, As, Pb, C, P and Ag		✓								Soil	350–700	(Cantrell et al. 2012)
Chicken manure and green waste biochar	Cd, Cu, Pb and Zn			✓			✓				Soil	550	(Park et al. 2011)
Cottonseed hulls biochar	Ni, Cu, Cd and Pb		✓	✓		✓	✓				Soil	200–800	(Uchimiya et al. 2011a)
DSTC	P			✓	✓						Water	600	(Yao et al. 2011a; Yao et al. 2011b)
Black carbon	C, H, N							✓			Soil	700/slow pyrolysis	(Heymann et al. 2011)

MPB manganese oxide-modified pine biochar, *BPB* birnessite-modified pine biochar, *ZVI* zerovalent iron, *MgEC* magnesium enriches biochar, *DAWC* digested dairy waste biochar, *DWSBC* digested whole sugar beet biochar, *DSTC* digested sugar beet tailing biochar

feedstocks at operating temperatures with a range of 350–600 °C. Solid state ^{13}C magic angle spinning (MAS) NMR spectra are obtained at a frequency off 100.6 MHz on a Varian Unity INOVA 400 NMR spectrometer. Carbon ssNMR spectra are attained by utilizing cross polarization (CP) as well as direct polarization (DP) techniques. There are some differences between corresponding CP and DP spectra. The broad alkyl signals at 15 and 35 ppm as well as carbohydrate signals in the range of 55–110 ppm, tend to be larger in the CP spectra. This indicates that carbohydrate and alkyl C are detected with greater efficiency than aromatic C by CP (McBeath et al. 2011). The observability of C (C_{obs}) in the biochar for the DP spectra ($C_{\text{obs}} - \text{DP} > 49\%$) is higher than for the CP spectra ($C_{\text{obs}} - \text{CP} < 61\%$). This can be partly attributed to the low ^1H content of the condensed aromatic units that form the bulk of char's molecular structure (McBeath et al. 2014). Ferromagnetic and paramagnetic, mainly iron minerals, can also affect NMR observability of charred materials. The iron contents are higher for the biochars produced from bamboo and food feedstocks, and this likely to have contributed to the very low CP for the bamboo and food at 600 °C biochars (Freitas et al. 2002).

The quantification of aromaticity from the ^{13}C NMR spectra of the different biochars is compromised by two main factors: (a) the presence of large spinning sidebands (*SSBs) that overlap with non-aromatic signal and (b) the low CP observability for all of the biochars and the low DP observability for a minority of the biochars as shown in Fig. 1. Aromaticity in biochar is generally easier to assess than the degree of aromatic condensation. In particular, the determination of elemental composition ($\text{O}-\text{C}_{\text{index}}$,

$\text{H}-\text{C}_{\text{index}}$), the spectroscopic assessment of functional groups ($\text{MIR}_{\text{index}}$, $\text{NEXAFS-aroma}_{\text{index}}$, $\text{NMR-aroma}_{\text{index}}$), the measurement of aromatic molecular markers ($\text{BPCA}_{\text{index}}$, $\text{PAH}_{\text{index}}$), and measuring the structural density ($\text{Pycno}_{\text{index}}$) can yield insight into the proportion of aromatic C in biochars (Wiedemeier et al. 2015).

However, there are glaring differences among these measures for biochars obtained at the similar temperature but subjecting dissimilar feedstocks. In this review, the study of different feedstocks (*chestnut*, *pinewood*, and *fescue*) shows that composition bears a dominant role in the chemical composition of the biochar, and this is also considered reasonably while evaluating the performance of biochar as a soil betterment and a C sink (Tables 2, 3). ssNMR spectra study of C demonstrates the influence of feedstock composition and yield temperature on the composition of aromatic portions in biochars, which further may be similar to be linked to their recalcitrance and ultimately their carbon sequestration value (McBeath et al. 2014; Wiedemeier et al. 2015).

Fourier transform infrared spectroscopy (ATR-FTIR)

FTIR is used for structural analysis and characterization of functional groups present on biochar surfaces. Structural analysis is performed using FTIR with a Bruker Vertex 70 spectrometer (Bruker Optics, Billerica, MA). This instrument is fitted with a MITacle attenuated total reflectance (ATR) accessory and with a diamond crystal plate. The spectra are obtained at 8 cm^{-1} resolution from 650 to 4500 cm^{-1} using a combined 128 scans (Cantrell et al.

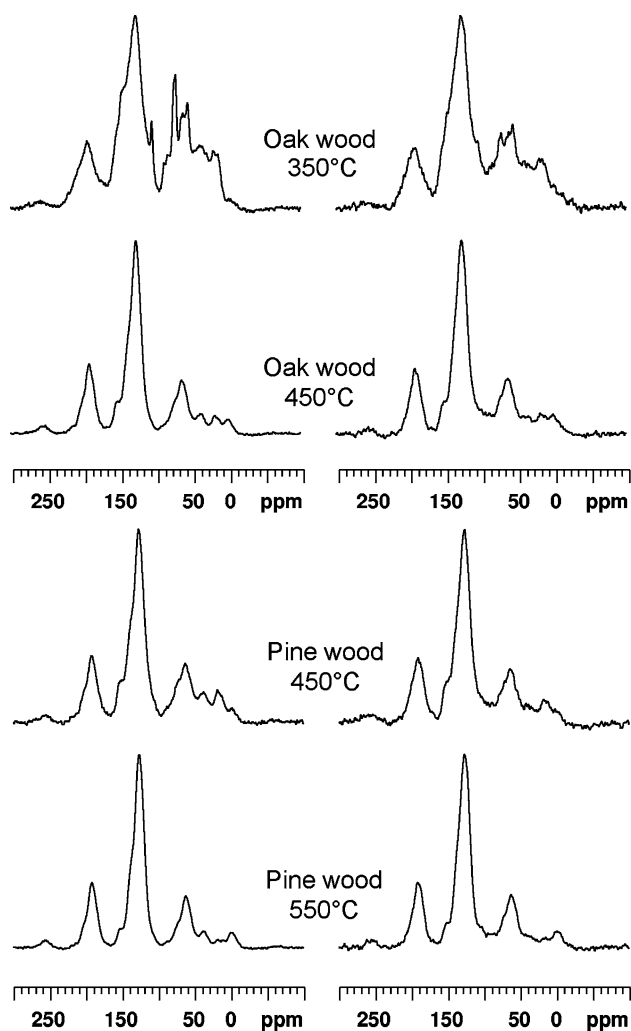


Fig. 1 Solid state ^{13}C CP and DP NMR spectra of biochars produced from wood feedstocks at production temperatures between 350 and 550 °C. Asterisks mark the position of spinning sidebands (SSBs) associated with the aromatic peak at 130 ppm. Note that the high-field SSB (ca. 65 ppm) may overlap with O-alkyl signal at the same chemical shift (McBeath et al. 2014), with permission from Elsevier

2012). All feedstocks and biochar samples are investigated before pretreatment. The FTIR spectral peak tasks are understood based on characteristic vibrations for those produced from wood and grass feedstock (Keiluweit et al. 2010), dairy manure (Cao and Harris 2010), bio-oil yielded during pyrolysis of manures occurring at higher rates (Xiu et al. 2010), natural organic matter (Wen et al. 2007), and bacterial surfaces (Jiang et al. 2004). The FTIR spectra are existing in supplementary matter for manure feedstocks and biochars generated at 350 and 700 °C such as soybean stover-derived biochar, iron-impregnated biochar (hickory), magnetic and nonmagnetic energy cane biochar, sugarcane bagasse and hickory wood biochar, sugarcane bagasse biochar, magnetic oak wood and bark biochar, biochar/MgAl-LDH (composites), DAWC and DWSBC, turkey litter biochar, and cottonseed hulls biochar (Table 3).

FTIR also describes the stretching of C–H bands that are associated with aliphatic functional groups. The presence of hydrocarbons is confirmed through FTIR for the better understanding of biochar structural properties. For the feedstocks, the broad band near 3300 cm^{-1} is attributed to the stretching vibration of H-bonded hydroxyl groups (Foo et al. 2012). The symmetric (2885 cm^{-1}) and asymmetric (2935 cm^{-1}) C–H (2870 cm^{-1}) stretching bands are linked with aliphatic functional groups. The C=O stretching for carboxyl, aldehyde, ester, and ketone are identified in the band width $1740\text{--}1700\text{ cm}^{-1}$. In addition to C=O stretching, vibrations bands for amides are noted at $1645\text{--}1653\text{ cm}^{-1}$ (Das et al. 2009). Absorption band of amide in this region likely results from carbonyl stretching vibration in the peptide bond, rather than the C–H stretching and N–H bending that appear at lower wave number (Jiang et al. 2004).

The FTIR analysis confirms the high quantity of N, O, and H, alkane, and cyclic alkene having functional groups on biochar surfaces, in addition with a strong peak that could denote sulfur, amine, or ester groups. Infrared spectroscopy is a promising technology that is used for different N functional groups in organic matter, in addition to being instantaneous and non-destructive. IR spectroscopy has been used to determine the relative amounts of protein, lignin, and carbohydrates in animal feeds. Mid-IR spectroscopy has been used to develop calibrations for N, C, and fiber contents in manure, for that, manure is scanned in the mid-infrared from 2500 to 25,000 nm ($4000\text{--}400\text{ cm}^{-1}$) on a DigiLab FTS 7000 FTIR spectrometer, using KBr as background reference (Calderón et al. 2006). This information reveals that the presence of nitrogen, oxygen, and iron-hydroxides groups/particles on the carbon surface tends to enhance the CO_2 , lead (Pb), (low temperature $200\text{--}400\text{ °C}$), antimony (Sb), cadmium (Cd), P, potassium (K), copper (Cu), nickel (Ni), C, silver (Ag), and arsenic (As) adsorption capacity in activated carbon (Fig. 2, 3). FTIR analyzes physicochemical variations and similarities. Recovery of biochar mass is correlated to the feedstock and C/N elemental properties. Percentage of nonvolatile minerals like P and K may prove to be beneficial for utilization of manure-based biochar as an alternative fertilizer (Cantrell et al. 2012).

Scanning electron microscopy (SEM)

SEM is mostly used for characterizing biochar and effective for detecting biochar macro-pores. However, microscopy and computerized tomography (CT) go through difficulties such as choosing representative samples and viewing orientations, development of image analysis protocols to quantify porosity, and definition of edges between solid and pore (Illingworth et al. 2013).

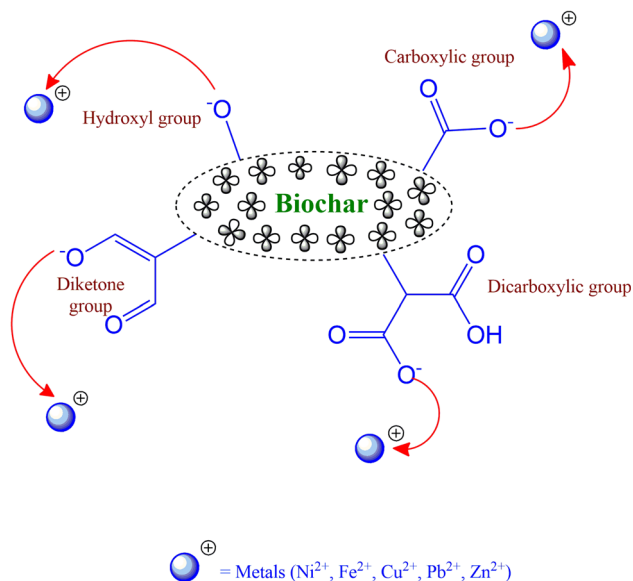


Fig. 2 Schematic sorption mechanism of metals ions on biochars

SEM is used to study the ultimate composition and surface morphology of biochars (composites) before and after sorption, such as iron-impregnated biochar (hickory), MPB and BPB, magnetic biochar (natural hematite, pinewood), magnetic and nonmagnetic energy cane biochar, ZVI biochar, clay biochar carbon composite, magnetic oak wood and bark biochar, MgEC, Biochar/MgAl-LDH (composites), biochar/ γ - Fe_2O_3 (composite), biochar/AIOOH nanocomposite, sewage sludge biochar, DAWC and DWSBC, MgO-biochar nanocomposite, chicken manure and green waste biochar, cottonseed hulls biochar, and DSTC for the removal of metals/non-metals, micro- and macronutrients and PAHs from soil and aqueous solution (Table 3). SEM images give the data of surface morphology, which is a significant factor in adsorbent-adsorbate connections. These elaborate that porous surfaces exist with a disorganized structural shape that still contains much of the wood cells original morphology. SEM has confirmed that residual wood cell and wood porosity morphologies remain significant features of the final biochar preparation (Mohan et al. 2015). The short residence time partially destroys the original wood cell morphology. The surface morphologies of the nanocomposites are non-smooth with some porosity due to the inherent nature of biochar (Zhang et al. 2012a). SEM has detected the soil black carbon occurrence as well as defined and amorphous particles. Lignocellulose biomass is converted from amorphous C structures to poly-aromatic graphene sheets with rising temperature, while low temperature BC is likely to be a complex combination of these two main C forms (Nguyen et al. 2010).

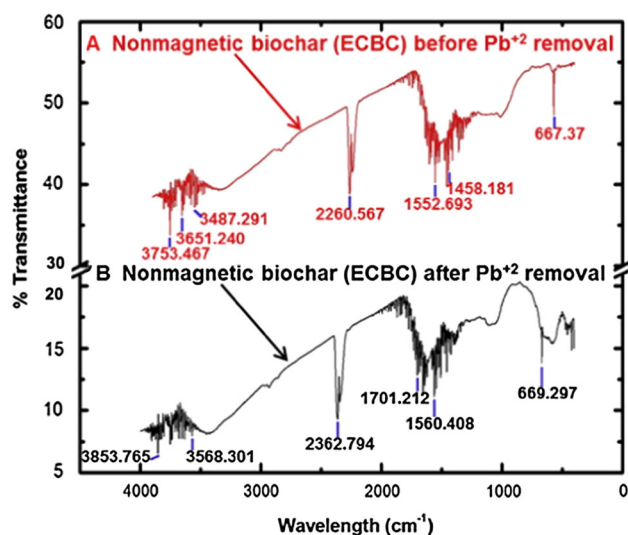


Fig. 3 FTIR spectra ($4000\text{--}500\text{ cm}^{-1}$) of energy cane biochar (ECBC) before and after lead adsorption. Energy cane biochar shows different oxygen containing surface groups ($\text{C}=\text{O}$, $\text{C}-\text{O}$, $-\text{OH}$), some olefins ($-\text{CH}_2$, $-\text{CH}_3$), and aromatic rings (Mohan et al. 2015), with permission from Elsevier

Transmission electron microscopy (TEM)

The TEM is exceptional for its quality to give data about size, morphology, composition, crystallinity, and electronic state of a sample, all with very high spatial resolution. Because a thin specimen is mandatory, specific sample preparation techniques such as ultra-microtomy, ion milling, or electro-polishing are sometimes needed. Tiny particles, fines, and colloidal suspensions are also dispersed on TEM grids oftenly. Seven biochar sorbents have been observed [magnetic and nonmagnetic energy cane biochar, magnetic oak wood and bark biochar, biochar/ γ - Fe_2O_3 (composite), biochar/AIOOH nanocomposite, MgO-Biochar nanocomposite, chicken manure and green waste biochar, and cottonseed hulls biochar] in this study (Table 3). To determine the surface microscopic identification of different biochar for the remediation of inorganic/organic substances (Pb, Cd, As, P, Nitrates, Cu, Zn, and Ni) with a 200-kV accelerating voltage TEM model JEOL 2100F (Japan) (Zhang et al. 2012b; Mohan et al. 2014b). This method could lead to improve a variety of adsorptive remediation processes.

X-rays photoelectron and Raman spectroscopy

XPS also referred as Electron spectroscopy for chemical analysis (ESCA) and it has been used in surface analysis because it can be applied to a higher range of materials and delivers valuable quantitative and chemical state information (Wu et al. 2012). XPS is typically proficient by

preparing the sample's surface to their excited state with mono-energetic Al $K\alpha$ X-rays causing photoelectrons which are released from the surface of the sample and an electron energy analyzer is used to compute the photoelectrons' energy released. Composition and speciation of surface elements of biochar samples are examined using XPS with a PHI 5100 series ESCA spectrometer (Perkin Elmer). The spectra of biochar and light fractions of the control and biochar amended soils shows two distinct peaks at ≈ 285.1 and 288.5 eV, which are attributed to the C $1s - \pi^*_{C=C}$ transitions of aromatic C and C $1s - \pi^*_{C=O}$ transitions of carboxylic C, carboxamide C, and carbonyl C. The proportion of aromatic C is higher in the light fraction of the (biochar produced at 550°C) amended soils than in the corresponding (biochar produced at 450°C) amended soils. XPS is the best tool for the analysis of the significant change in the proportion of aromatic C of fresh and aged biochar (Singh et al. 2014).

Furthermore, the increased carbon defect population perceived by XPS gives an additional support to the Raman findings (Li et al. 2011). Raman spectroscopy is very valuable tool for the characterization of carbon-based nanostructures. The Raman spectra of pristine and treated multi-walled nanotubes is excited with the range of 514.5 nm laser line. It consists of three characteristic bands, namely the D band at approximately 1338 cm^{-1} , which shows the presence of amorphous carbon in the samples, the G band which originates from tangible stretching of the carbon-carbon bonds in graphene sheet and the D band which is a weak part of the G band (Datyuk et al. 2008). In this review, four biochar materials have been derived from the different feedstocks, such as iron-impregnated biochar (hickory), MPB and BPB, magnetic biochar (natural hematite, pinewood), and biochar/ γ - Fe_2O_3 (composite) as shown in Table 3. The effect of initial Pb ion concentration and the adsorption isotherms is also examined to compare the adsorption characteristics and mechanism of Pb ion on the different mesoporous biochars and after modification (Li et al. 2016). The mechanism of Pb and As sorption on the iron-impregnated biochar are further discovered using a characterization tool XPS (Fig. 4), to set a modest and easy way to activate method for cost-efficient sorbents yield and removal ability, and determine the sorption mechanism of metals by surface analysis. For the further examination of metal sorption mechanism of the different metal-impregnated biochars, binding energy shifts for carbon, iron, oxygen, and metals can be observed using XPS (Hu et al. 2015).

X-rays diffractometer (XRD)

XRD examines crystalline material structure and size. For that a computer controlled X-rays diffractometer, equipped

with a stepping motor, a graphite crystal monochromator and a $\text{Cu}K\alpha$ radiation source are used. XRD analysis provides, analysis of solids, powders and liquids reflection and small angle X-rays scattering (SAXS). The XRD patterns of magnetic oak bark and wood biochars are obtained on a powder XRD system from the PANalytical model X'Pert PRO using $\text{Cu} K\alpha$ ($k = 1.54 \text{ \AA}$) radiation at 45 kV and 40 mA (Jia et al. 2007). As grain size decreases, hardness would be increases and peaks become broader. The particle size of MgO and $\text{Mg}(\text{OH})_2$ within the biochar matrix and width of the XRD peaks are calculated using the Debye-Scherrer equation which is designed in 1918 for determination of the mean size of single-crystal nanoparticles or crystallite in nanocrystalline bulk materials in the form as (Holzwarth and Gibson 2011).

$$l = \frac{K\lambda}{\beta \cos \theta}, \quad (1)$$

where K is the shape factor with a value of about 0.9, λ is the X-ray wavelength, β is the line broadening at half the maximum intensity (FWHM) in radians, and θ is the Bragg angle; l is the mean size of the ordered (crystalline) domain. Using the X-ray diffraction techniques and Bragg's law to derive the structure of crystals and show the exact position of atoms (converts angle to distance).

$$\eta\lambda = 2d \cdot \sin \theta, \quad (2)$$

where η is an integer determined by the order given, λ is the wavelength of X-rays, d is the spacing between the planes in the atomic lattice, and θ is the angle between the incident ray and scattering planes (Yao et al. 2013).

The sorption mechanism of As, Pb, Ag, Cr^{6+} , Cd, P, Co, Cu, Ni, Zn, PAHs, K, and NO_3^- on the fifteen biochars [iron-impregnated biochar (hickory), MPB and BPB, magnetic biochar (natural hematite, pinewood), magnetic and nonmagnetic energy cane biochar, ZVI biochar, clay biochar carbon composite, magnetic oak wood and bark biochar, MgEC, biochar/MgAl-LDH (Composites), biochar/ γ - Fe_2O_3 (composite), biochar/ AlOOH nanocomposite, sewage sludge biochar, DAWC and DWSBC, MgO-biochar nanocomposite, and DSTC] as shown in Fig. 2, has been further explored using a characterization tool XRD to develop a way for preparation of cost-effective sorbents that estimates the removal ability of different inorganic/organic substances (Table 3).

Some unknown peaks emerged in the XRD pattern, signifying the existence of a small amount of other minerals, which are commonly detected for biochars formed from agriculture and forest residues at high pyrolytic temperatures (Inyang et al. 2012). With the increase of reaction time, noticeable changes in the relative intensities of the XRD peaks are observed and the diffraction peak becomes stronger and stronger. The strong and sharp XRD

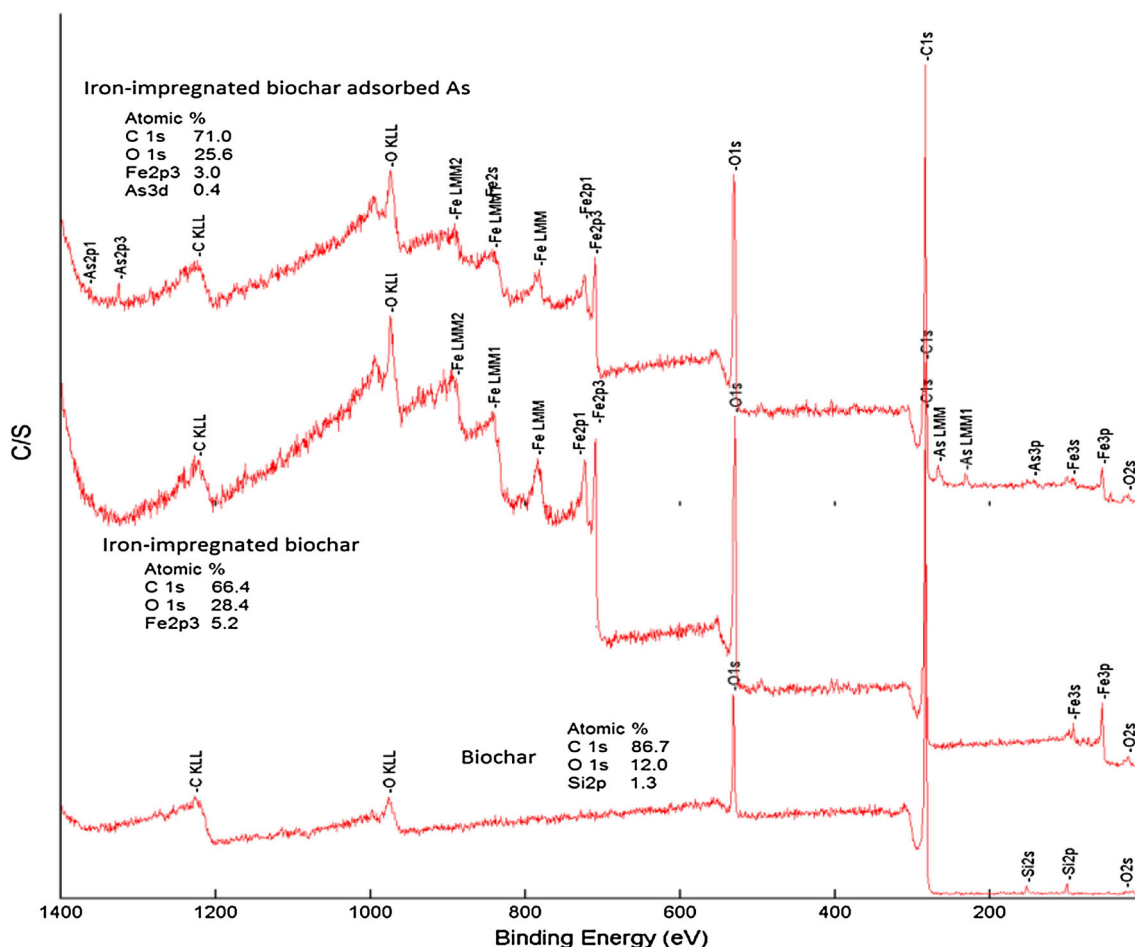


Fig. 4 XPS analysis of pristine biochar and the pre- and post-sorption Fe-impregnated biochar, binding energy shift for carbon, oxygen, iron, and arsenic are examined. Seven prominent Fe peaks corresponding to Fe_{3p} , Fe_{3s} , Fe_{2p1} , Fe_{2p3} , Fe LMM, Fe LMM1, and Fe

LMM2 and As peaks corresponding to As_{3p} , As_{3s} , As_{2p1} , As_{2p3} , As LMM, and As LMM1 are found in the surface of Fe-impregnated biochar both before and after As interaction (Hu et al. 2015), with permission from Elsevier

peaks suggest the as-prepared fractal nanocrystals are well crystallized. Such variations may be due to the diameter of the produced particles is getting larger with the increase of time (Zhang and Gao 2013). XRD is very helpful for the preparation of fast, easy, and non-destructive sample of biochar, with the high accuracy for d-spacing calculations and single crystal, poly and amorphous materials (Fig. 5).

Thermogravimetric and derivative thermogravimetric analysis (TGA-DTG)

TGA in actual sense is applicable for thermal analysis in which changes in physical and chemical properties of materials are measured as a function of increasing temperature. Temperature can be responsible for data about physical changes, such as phase transitions (Yao et al. 2014). TGA was carried out at a heating rate of 10 °C/min using a Mettler's TGA/DSC thermogravimetric analyzer under a stream of air at 25–700 °C to study the

thermal stability of biochar. Adsorption kinetics of CO_2 is determined using a TGA instrument at flow rate of 50 ml/min. It is found that the existence of N_2 functionalities on C surface generally enhanced the CO_2 adsorption capacity. It is important to reference that the elemental analysis here only analyzes the N_2 , C, S, and H_2 content of carbon. The O_2 content is assessed by difference assuming that only five elements C, H, N, S, and O could be gasified from carbon samples. Proximate analysis is carried out with the aid of TGA to determine the amount of ash and volatile matter (Shafeeyan et al. 2011). The pyrolysis characteristics are described via TG and derivative thermogravimetric (DTG) curve of raw biomass under anaerobic conditions. The variations in elemental composition and the decomposition process of raw biomass in TG-DTG, specifying that increasing pyrolytic temperature produces biochar with decreases in surface acidity, polarity, and the increase in the aromaticity (Fig. 6; Kim et al. 2013).

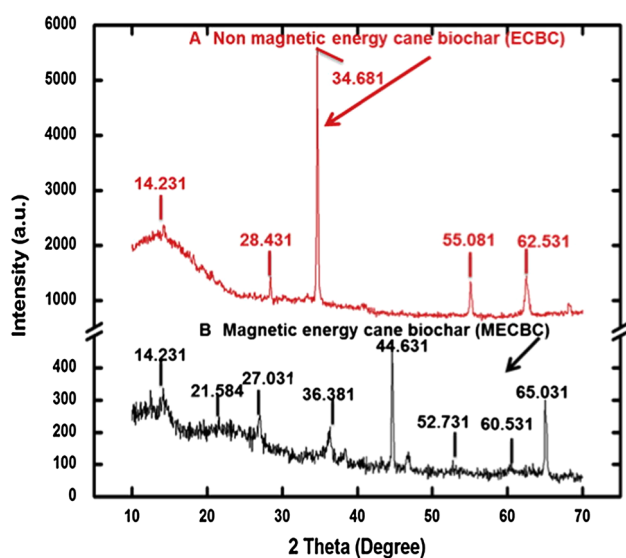


Fig. 5 XRD spectra of (a) nonmagnetic energy cane biochar (ECBE) and (b) magnetic energy cane biochar (MECBC). Magnetic biochar gave multiple peaks in the 20°–90° 2 θ range, confirming crystalline regions due to various Fe₂O₃ species. Peak at 27.02° exhibits Lepidocrocite's FeOOH, i.e., formed by the oxidation of Fe(III), and peak at 46.73° is also due to FeOOH, while the peak at 38.26° is owing to the presence of γ -Fe₂O₃ (Mohan et al. 2015), with permission from Elsevier

Total ten sorbents [woody feedstock biochar (pine, grass species, and citrus), iron-impregnated biochar (hickory), magnetic biochar (natural hematite, pinewood), ZVI biochar, sugarcane bagasse and hickory wood biochar, clay biochar carbon composite (slow pyrolysis), magnetic oak wood and bark biochar, MgEC, MgO biochar nanocomposite, and cottonseed hulls biochar] have been studied for the better understanding of adsorption kinetics of various substances, such as As, Pb, Ag, Cr⁶⁺, CO₂, P, Ni, Cu, and Cd as shown in Fig. 2. The water-holding capacity of the biochar is further evaluated with TG analyses of the water-saturated biochars (Wang et al. 2015b). Through the various information that obtained from TG analysis, tells the story of stability of different samples of biochar. These results further confirm the association of the metal particles with biochar surfaces as shown in Table 3.

Near edge X-ray absorption fine structure spectroscopy (NEXAFS)

In soil biogeochemistry, black carbon has a significant role. Its complexity, mainly within environmental matrices, presents a challenge for researchers, primarily as a result of techniques which may favor the detection of certain functional group types instead of capturing total sample carbon. To utilize C 1s-NEXAFS to characterize the C chemistry and functional groups of a broad range of black carbon

(BC) and feedstocks (chestnut, pinewood, and fescue) materials. Characteristic resonance in the NEXAFS spectra showed direct molecular speciation of the total carbon chemistry of the potentially interfering and reference materials and environmental matrices that are obtained from an earlier BC and different feedstock trial. NEXAFS shows high aromaticity values at low temperature range for unaltered feedstocks and showing decreasing aromaticity with increasing temperature. BC reference materials and soils were categorized by an aromatic C region containing around 40 % of total absorption intensity; however, some limitations of the technique were addressed (Wiedemeier et al. 2015).

Analytical technique for PAHs analysis

GC–MS analyses have been accomplished by utilization of 7890A gas chromatograph which is in connection to a 5975C mass spectrometer (Agilent, Santa Clara, CA, USA). Capillary column HP- 5MS (length: 30 m; inner diameter: 0.25 mm; thickness: 0.25 μ m) is applied (Hewlett–Packard, Wilmington, DE, USA). The temperature gradient at operating situations of the GC–MS is 50 °C isotherm for 1 min, 20 °C min⁻¹ to 200 °C, 5 °C min⁻¹ to 310 °C, and isotherm for 10 min. The MS is run in the electron ionization mode (70 eV), and acquisition is done using single-ion monitoring at the molecular ion of each PAHs at the time windows analogous to their retention times. In this review, two feedstocks have been considered, (1) wheat straw biochar produced at slow pyrolysis (2) and soil amended PAHs biochar produced by combining homogenized biochar with a biological compound fertilizer at a 50 % (w/w) ratio to develop a non-toxic/non-hazardous solvent mixture (1:1 acetone:cyclohexane) instead of toxic/hazardous solvents (e.g., dichloromethane, toluene), for GS-MS analysis as shown in Table 3. This study delivered a novel and proficient method for extraction of PAHs from slow pyrolysis produced biochar and char-based fertilizers (Chen et al. 2015). Furthermore, this technique provides acceptable PAHs recovery when introduced to a wide range of biochar samples attained at different pyrolysis conditions, using different biomass materials, signifying, this analytical practice could be used effectively on different biochars.

This review summarizes and evaluates biochar identification methods, corresponding mechanisms, and their benefits for contaminant management in soil and water. Identification of biochar through modern analytical techniques is likely to result in variations in its surface properties including surface area, surface charge, functional groups, and pore volume and distribution. Applicability and performance of modify methods depend upon the type of contaminants (i.e., polar/non-polar, anionic/cationic,

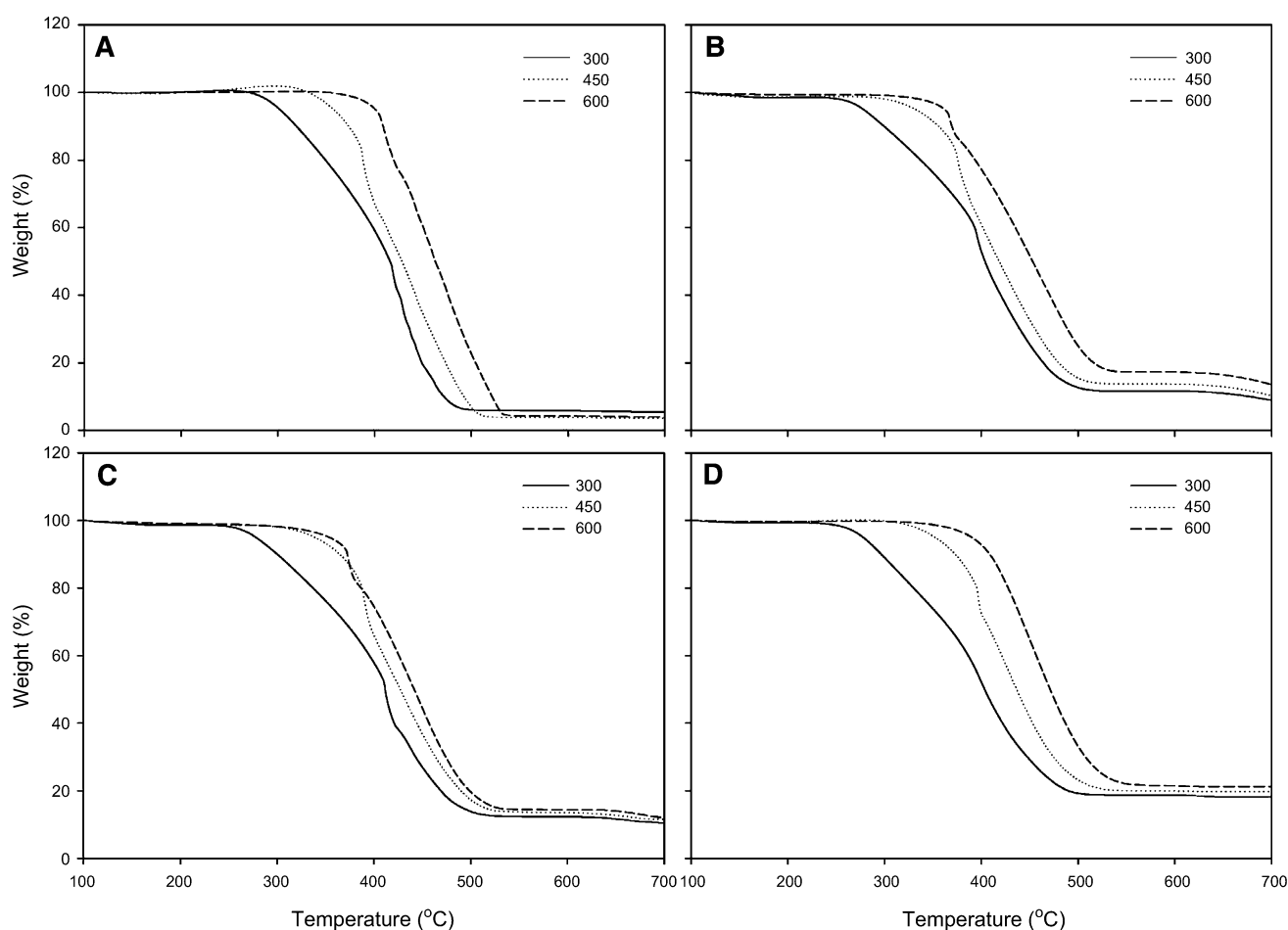


Fig. 6 Thermogravimetric curves of biochars derived from pinewood (**a**), citrus wood (**b**), alfalfa (**c**), and switchgrass (**d**) (Wang et al. 2015b), with permission from Elsevier

hydrophilic/hydrophobic, and inorganic/organic), environmental conditions, remediation goals, and land use purpose in general. The conclusive remarks for this section are that all discussed techniques are standard for biochar characterization. Some of them are used to observe the morphological-related parameters such as XRD, TEM, and SEM, whereas some focus on chemical composition of biochar such as XPS, ATR-FTIR, ssNMR, and GC-MS. Among these techniques XPS, FTIR, SEM, and TEM are more common and relied techniques. Although it is determined that regardless the production cost is significantly reduced in the meantime due to the improvements in technology, the cost of biochar remains high due to lack of production and high demand.

Conclusion and recommendations

In this study, all analytical techniques are discussed comprehensively which may be applicable for better understanding of structural, physical, and chemical properties of biochar. The mechanism of biochar function in soil, which

appears to be sensitive to conditions prevailing during its formation, are also affected by the material from which it is produced. Biochar potentially impacts on soil health and functions and interacts with many soil properties, because of the wide range of effects from biochar addition to soil. To control biomass and product (biochar) quality, a standard set of analytical methods and procedures are necessary. ssNMR, ATR-FTIR, SEM, TEM, XPS, XRD, TGA-DTG, NEXAFS, and GC-MS analyses proposed that carbon on surface of the biochar played an important role in sorption of targeted substances. The sorption process was controlled through the chemisorption mechanism for enhancing the soil fertility, storing carbon, and cation exchange ability which play useful environmental functions. All techniques did a good job of measuring increased capacity, surface area, and activity for the different biochars. Previously none of the researchers has imparted coverage to all of the above techniques simultaneously. Present study consists of unanimous discussion of all these techniques, which will make it easy and helpful for the research in future. Therefore, all the discussed techniques

are found to have a greater significance as being helpful in accurate characterization of biochar, which in turn is not given ignorance during its utilization/application, that is beneficial not only for environment but also for agriculture.

References

- Ahmad M, Usman AR, Lee SS et al (2012) Eggshell and coral wastes as low cost sorbents for the removal of Pb^{2+} , Cd^{2+} and Cu^{2+} from aqueous solutions. *J Ind Eng Chem* 18:198–204. doi:10.1016/j.jiec.2011.11.013
- Ahmad M, Rajapaksha AU, Lim JE et al (2014) Biochar as a sorbent for contaminant management in soil and water: a review. *Chemosphere* 99:19–23. doi:10.1016/j.chemosphere.2013.10.071
- Alper K, Tekin K, Karagöz S (2014) Pyrolysis of agricultural residues for bio-oil production. *Clean Technol Environ Policy* 17:211–223. doi:10.1007/s10098-014-0778-8
- Beesley L, Moreno-Jiménez E, Gomez-Eyles JL et al (2011) A review of biochars' potential role in the remediation, revegetation and restoration of contaminated soils. *Environ Pollut* 159:3269–3282. doi:10.1016/j.envpol.2011.07.023
- Brewer CE, Chuang VJ, Masiello C et al (2014) New approaches to measuring biochar density and porosity. *Biomass Bioenergy* 66:176–185. doi:10.1016/j.biombioe.2014.03.059
- Bruun EW, Hauggaard-Nielsen H, Ibrahim N et al (2011) Influence of fast pyrolysis temperature on biochar labile fraction and short-term carbon loss in a loamy soil. *Biomass Bioenergy* 35:1182–1189. doi:10.1016/j.biombioe.2010.12.008
- Calderón FJ, McCarty GW, Reeves JB (2006) Pyrolysis-MS and FT-IR analysis of fresh and decomposed dairy manure. *J Anal Appl Pyrolysis* 76:14–23. doi:10.1016/j.jaap.2005.06.009
- Cantrell KB, Hunt PG, Uchimiya M et al (2012) Impact of pyrolysis temperature and manure source on physicochemical characteristics of biochar. *Bioresour Technol* 107:419–428. doi:10.1016/j.biortech.2011.11.084
- Cao X, Harris W (2010) Properties of dairy manure derived biochar pertinent to its potential use in remediation. *Bioresour Technol* 101:5222–5228. doi:10.1016/j.biortech.2010.02.052
- Cao X, Ma L, Liang Y et al (2011) Simultaneous immobilization of lead and atrazine in contaminated soils using dairy-manure biochar. *Environ Sci Technol* 45:4884–4889. doi:10.1021/es103752u
- Charon E, Rouzaud JN, Aléon J (2014) Graphitization at low temperatures in the presence of iron implications in planetology. *Carbon N Y* 66:178–190. doi:10.1016/j.carbon.2013.08.056
- Chen P, Sun M, Zhu Z et al (2015) Optimization of ultrasonic-assisted extraction for determination of polycyclic aromatic hydrocarbons in biochar-based fertilizer by gas chromatography–mass spectrometry. *Anal Bioanal Chem* 407:6149–6157. doi:10.1007/s00216-015-8790-3
- Cheng CH, Lehmann J (2009) Ageing of black carbon along a temperature gradient. *Chemosphere* 75:1021–1027. doi:10.1016/j.chemosphere.2009.01.045
- Chintala R, Mollinedo J, Schumacher TE et al (2013) Effect of biochar on chemical properties of acidic soil. *Arch Agron Soil Sci* 60:393–404. doi:10.1080/03650340.2013.789870
- Chintala R, Schumacher TE, McDonald LM et al (2014) Phosphorus sorption and availability from biochars and soil/biochar mixtures. *CLEAN Soil Air Water* 42:626–634. doi:10.1002/clen.201300089
- Cordero T, Marquez F, Rodríguez-Mirasol J, Rodríguez J (2001) Predicting heating values of lignocellulosics and carbonaceous materials from proximate analysis. *Fuel* 80:1567–1571. doi:10.1016/S0016-2361(01)00034-5
- Cowie AL, Downie AE, George BH et al (2012) Is sustainability certification for biochar the answer to environmental risks? *Pesqui Agropecu Bras* 47:637–648. doi:10.1590/S0100-204X2012000500002
- Creamer AE, Gao B, Zhang M (2014) Carbon dioxide capture using biochar produced from sugarcane bagasse and hickory wood. *Chem Eng J* 249:174–179. doi:10.1016/j.cej.2014.03.105
- Das DD, Schnitzer MI, Monreal CM, Mayer P (2009) Chemical composition of acid-base fractions separated from bio oil derived by fast pyrolysis of chicken manure. *Bioresour Technol* 100:6524–6532. doi:10.1016/j.biortech.2009.06.104
- Datsyuk V, Kalyva M, Papagelis K et al (2008) Chemical oxidation of multiwalled carbon nanotubes. *Carbon N Y* 46:833–840. doi:10.1016/j.carbon.2008.02.012
- Dempster DN, Gleeson DB, Solaiman ZM et al (2012) Decreased soil microbial biomass and nitrogen mineralisation with Eucalyptus biochar addition to a coarse textured soil. *Plant Soil* 354:311–324. doi:10.1007/s11104-011-1067-5
- Ding W, Dong X, Ime IM et al (2014) Pyrolytic temperatures impact lead sorption mechanisms by bagasse biochars. *Chemosphere* 105:68–74. doi:10.1016/j.chemosphere.2013.12.042
- Enders A, Hanley K, Whitman T et al (2012) Characterization of biochars to evaluate recalcitrance and agronomic performance. *Bioresour Technol* 114:644–653. doi:10.1016/j.biortech.2012.03.022
- Fabbri D, Rombolà AG, Torri C, Spokas KA (2013) Determination of polycyclic aromatic hydrocarbons in biochar and biochar amended soil. *J Anal Appl Pyrolysis* 103:60–67. doi:10.1016/j.jaap.2012.10.003
- Feng Y, Xu Y, Yu Y et al (2012) Mechanisms of biochar decreasing methane emission from Chinese paddy soils. *Soil Biol Biochem* 46:80–88. doi:10.1016/j.soilbio.2011.11.016
- Foo LPY, Tee CZ, Raimy NR et al (2012) Potential Malaysia agricultural waste materials for the biosorption of cadmium(II) from aqueous solution. *Clean Technol Environ Policy* 14:273–280. doi:10.1007/s10098-011-0398-5
- Freitas JCC, Passamani EC, Orlando MTD et al (2002) Effects of ferromagnetic inclusions on ^{13}C MAS NMR spectra of heat treated peat samples. *Energy Fuels* 16:1068–1075. doi:10.1021/ef010283w
- Gaskin JW, Steiner C, Harris K et al (2008) Effect of low temperature pyrolysis conditions on biochar for agricultural use. *Trans ASABE* 51:2061–2069. doi:10.13031/2013.25409
- Glaser B, Lehmann J, Zech W (2002) Ameliorating physical and chemical properties of highly weathered soils in the tropics with charcoal: a review. *Biol Fertil Soils* 35:219–230. doi:10.1007/s00374-002-0466-4
- Heymann K, Lehmann J, Solomon D et al (2011) C 1 s K-edge near edge X-ray absorption fine structure (NEXAFS) spectroscopy for characterizing functional group chemistry of black carbon. *Org Geochem* 42:1055–1064. doi:10.1016/j.orggeochem.2011.06.021
- Hiller E, Fargasová A, Zemanová L, Bartal M (2008) Influence of wheat ash on the MCPA immobilization in agricultural soils. *Bull Environ Contam Toxicol* 81:285–288. doi:10.1007/s00128-008-9400-2
- Holzwarth U, Gibson N (2011) The Scherrer equation versus the “Debye–Scherrer equation”. *Nat Nanotechnol* 6:534. doi:10.1038/nnano.2011.145
- Hossain MK, Strezov Vladimir V, Chan KY et al (2011) Influence of pyrolysis temperature on production and nutrient properties of wastewater sludge biochar. *J Environ Manag* 92:223–228. doi:10.1016/j.jenvman.2010.09.008
- Hu X, Ding Z, Zimmerman AR et al (2015) Batch and column sorption of arsenic onto iron-impregnated biochar synthesized

- through hydrolysis. *Water Res* 68:206–216. doi:[10.1016/j.watres.2014.10.009](https://doi.org/10.1016/j.watres.2014.10.009)
- Huisman DJ, Braadbaart F, van Wijk IM, van Os BJH (2012) Ashes to ashes, charcoal to dust: micromorphological evidence for ash-induced disintegration of charcoal in Early Neolithic (LBK) soil features in Elsloo (The Netherlands). *J Archaeol Sci* 39:994–1004. doi:[10.1016/j.jas.2011.11.019](https://doi.org/10.1016/j.jas.2011.11.019)
- Inyang M, Gao B, Yao Y et al (2012) Removal of heavy metals from aqueous solution by biochars derived from anaerobically digested biomass. *Bioresour Technol* 110:50–56. doi:[10.1016/j.biortech.2012.01.072](https://doi.org/10.1016/j.biortech.2012.01.072)
- Ippolito J, Novak JM, Busscher WJ et al (2012) Switchgrass biochar affects two aridisols. *J Environ Qual* 41:1123–1130. doi:[10.2134/jeq2011.0100](https://doi.org/10.2134/jeq2011.0100)
- Jaafar NM, Clode PL, Abbott LK (2014) Microscopy observations of habitable space in biochar for colonization by fungal hyphae from soil. *J Integr Agric* 13:483–490. doi:[10.1016/S2095-3119\(13\)60703-0](https://doi.org/10.1016/S2095-3119(13)60703-0)
- Jia Y, Xu L, Wang X, Demopoulos GP (2007) Infrared spectroscopic and X-rays diffraction characterization of the nature of adsorbed arsenate on ferrihydrite. *Geochim Cosmochim Acta* 71:1643–1654. doi:[10.1016/j.gca.2006.12.021](https://doi.org/10.1016/j.gca.2006.12.021)
- Jiang W, Saxena A, Song B et al (2004) Elucidation of functional groups on gram-positive and gram-negative bacterial surfaces using infrared spectroscopy elucidation of functional groups on gram-positive and gram-negative bacterial surfaces using infrared spectroscopy. *Langmuir* 20:11433–11442. doi:[10.1021/la049043](https://doi.org/10.1021/la049043)
- Karhu K, Mattila T, Bergström I, Regina K (2011) Biochar addition to agricultural soil increased CH₄ uptake and water holding capacity: results from a short-term pilot field study. *Agric Ecosyst Environ* 140:309–313. doi:[10.1016/j.agee.2010.12.005](https://doi.org/10.1016/j.agee.2010.12.005)
- Keiluweit M, Nico PS, Johnson MG, Kleber M (2010) Dynamic molecular structure of plant biomass-derived black carbon (biochar). *Environ Sci Technol* 44:1247–1253. doi:[10.1021/es9031419](https://doi.org/10.1021/es9031419)
- Khan S, Wang N, Reid BJ et al (2013) Reduced bioaccumulation of PAHs by *Lactuca sativa* L. grown in contaminated soil amended with sewage sludge and sewage sludge derived biochar. *Environ Pollut* 175:64–68. doi:[10.1016/j.envpol.2012.12.014](https://doi.org/10.1016/j.envpol.2012.12.014)
- Khan S, Reid BJ, Li G, Zhu Y-G (2014) Application of biochar to soil reduces cancer risk via rice consumption: a case study in Miaojian village, Longyan, China. *Environ Int* 68:154–161. doi:[10.1016/j.envint.2014.03.017](https://doi.org/10.1016/j.envint.2014.03.017)
- Kim WK, Shim T, Kim YS et al (2013) Characterization of cadmium removal from aqueous solution by biochar produced from a giant Miscanthus at different pyrolytic temperatures. *Bioresour Technol* 138:266–270. doi:[10.1016/j.biortech.2013.03.186](https://doi.org/10.1016/j.biortech.2013.03.186)
- Lashari MS, Ye Y, Ji H et al (2014) Biochar-manure compost in conjunction with pyroligneous solution alleviated salt stress and improved leaf bioactivity of maize in a saline soil from central China: a 2-year field experiment. *J Sci Food Agric*. doi:[10.1002/jsfa.6825](https://doi.org/10.1002/jsfa.6825)
- Lehmann J, Joseph S (2009) Biochar for environmental management: science and technology, 1st edn. EARTHSCAN, Gateshead
- Li P, Jiang EY, Bai HL (2011) Fabrication of ultrathin epitaxial γ -Fe₂O₃ films by reactive sputtering. *Phys D Appl Phys*. doi:[10.1088/0022-3727/44/7/075003](https://doi.org/10.1088/0022-3727/44/7/075003)
- Li K, Jiang Y, Wang X et al (2016) Effect of nitric acid modification on the lead(II) adsorption of mesoporous biochars with different mesopore size distributions. *Clean Technol Environ Policy* 18:797–805. doi:[10.1007/s10098-015-1056-0](https://doi.org/10.1007/s10098-015-1056-0)
- Lian F, Huang F, Chen W et al (2011) Sorption of apolar and polar organic contaminants by waste tire rubber and its chars in single- and bi-solute systems. *Environ Pollut* 159:850–857. doi:[10.1016/j.envpol.2011.01.002](https://doi.org/10.1016/j.envpol.2011.01.002)
- Illingworth J, Williams PT, Rand B (2013) Characterisation of biochar porosity from pyrolysis of biomass flax fibre. *J Energy Inst* 86(2):63–70. doi:[10.1179/1743967112Z.00000000046](https://doi.org/10.1179/1743967112Z.00000000046)
- Lou L, Luo L, Yang Q et al (2012) Release of pentachlorophenol from black carbon-inclusive sediments under different environmental conditions. *Chemosphere* 88:598–604. doi:[10.1016/j.chemosphere.2012.03.039](https://doi.org/10.1016/j.chemosphere.2012.03.039)
- Maroušek J (2014) Significant breakthrough in biochar cost reduction. *Clean Technol Environ Policy* 16:1821–1825. doi:[10.1007/s10098-014-0730-y](https://doi.org/10.1007/s10098-014-0730-y)
- McBeath AV, Smernik RJ, Schneider MPW et al (2011) Determination of the aromaticity and the degree of aromatic condensation of a thermosequence of wood charcoal using NMR. *Org Geochem* 42:1194–1202. doi:[10.1016/j.orggeochem.2011.08.008](https://doi.org/10.1016/j.orggeochem.2011.08.008)
- McBeath AV, Smernik RJ, Krull ES, Lehmann J (2014) The influence of feedstock and production temperature on biochar carbon chemistry: a solid-state ¹³C NMR study. *Biomass Bioenergy* 60:121–129. doi:[10.1016/j.biombioe.2013.11.002](https://doi.org/10.1016/j.biombioe.2013.11.002)
- Mohan D, Pittman CU, Bricka M et al (2007) Sorption of arsenic, cadmium, and lead by chars produced from fast pyrolysis of wood and bark during bio-oil production. *J Colloid Interface Sci* 310:57–73. doi:[10.1016/j.jcis.2007.01.020](https://doi.org/10.1016/j.jcis.2007.01.020)
- Mohan D, Kumar H, Sarswat A et al (2014a) Cadmium and lead remediation using magnetic oak wood and oak bark fast pyrolysis bio-chars. *Chem Eng J* 236:513–528. doi:[10.1016/j.cej.2013.09.057](https://doi.org/10.1016/j.cej.2013.09.057)
- Mohan D, Sarswat A, Ok YS, Pittman CU (2014b) Organic and inorganic contaminants removal from water with biochar, a renewable, low cost and sustainable adsorbent: a critical review. *Bioresour Technol* 160:191–202. doi:[10.1016/j.biortech.2014.01.120](https://doi.org/10.1016/j.biortech.2014.01.120)
- Mohan D, Singh P, Sarswat A et al (2015) Lead sorptive removal using magnetic and nonmagnetic fast pyrolysis energy cane biochars. *J Colloid Interface Sci* 448:238–250. doi:[10.1016/j.jcis.2014.12.030](https://doi.org/10.1016/j.jcis.2014.12.030)
- Morales VL, Pérez-Reche FJ, Hapca SM et al (2015) Reverse engineering of biochar. *Bioresour Technol* 183:163–174. doi:[10.1016/j.biortech.2015.02.043](https://doi.org/10.1016/j.biortech.2015.02.043)
- Mukherjee A, Zimmerman AR, Harris W (2011) Surface chemistry variations among a series of laboratory-produced biochars. *Geoderma* 163:247–255. doi:[10.1016/j.geoderma.2011.04.021](https://doi.org/10.1016/j.geoderma.2011.04.021)
- Nartey OD, Zhao B (2014) Biochar preparation, characterization, and adsorptive capacity and its effect on bio availability of contaminants: an overview. *Adv Mater Sci Eng* 2014:1–12. doi:[10.1155/2014/715398](https://doi.org/10.1155/2014/715398)
- Nguyen BT, Lehmann J, Hockaday WC et al (2010) Temperature sensitivity of black carbon decomposition and oxidation. *Environ Sci Technol* 44:3324–3331. doi:[10.1021/es903016y](https://doi.org/10.1021/es903016y)
- Novak JM, Busscher WJ (2013) *Advanced biofuels and bioproducts*. Springer, New York, pp 69–96. doi:[10.1007/978-1-4614-3348-4_7](https://doi.org/10.1007/978-1-4614-3348-4_7)
- Novak JM, Busscher WJ, Laird DL et al (2009) Impact of biochar amendment on fertility of a Southeastern coastal plain soil. *Soil Sci* 174:105–112. doi:[10.1097/SS.0b013e3181981d9a](https://doi.org/10.1097/SS.0b013e3181981d9a)
- Park JH, Choppala GK, Bolan NS et al (2011) Biochar reduces the bioavailability and phytotoxicity of heavy metals. *Plant Soil* 348:439–451. doi:[10.1007/s11104-011-0948-y](https://doi.org/10.1007/s11104-011-0948-y)
- Petit C, Kante K, Bandosz TJ (2010) The role of sulfur-containing groups in ammonia retention on activated carbons. *Carbon N Y* 48:654–667. doi:[10.1016/j.carbon.2009.10.007](https://doi.org/10.1016/j.carbon.2009.10.007)
- Rajkovich S, Enders A, Hanley K et al (2012) Corn growth and nitrogen nutrition after additions of biochars with varying properties to a temperate soil. *Biol Fertil Soils* 48:271–284. doi:[10.1007/s00374-011-0624-7](https://doi.org/10.1007/s00374-011-0624-7)
- Razon LF (2014) Is nitrogen fixation (once again) “vital to the progress of civilized humanity”? *Clean Technol Environ Policy*. doi:[10.1007/s10098-014-0835-3](https://doi.org/10.1007/s10098-014-0835-3)

- Rutigliano FA, Romano M, Marzaioli R et al (2014) Effect of biochar addition on soil microbial community in a wheat crop. *Eur J Soil Biol* 60:9–15. doi:10.1016/j.ejsobi.2013.10.007
- Shafeeyan MS, Daud WMAW, Houshmand A, Arami-Niya A (2011) Ammonia modification of activated carbon to enhance carbon dioxide adsorption: effect of pre-oxidation. *Appl Surf Sci* 257:3936–3942. doi:10.1016/j.apsusc.2010.11.127
- Singh B, Fang Y, Cowie BCC, Thomsen L (2014) NEXAFS and XPS characterisation of carbon functional groups of fresh and aged biochars. *Org Geochem* 77:1–10. doi:10.1016/j.orggeochem.2014.09.006
- Spokas KA, Novak JM, Venterea RT (2012) Biochar's role as an alternative N-fertilizer: ammonia capture. *Plant Soil* 350:35–42. doi:10.1007/s11104-011-0930-8
- Tong XJ, Li JY, Yuan JH, Xu RK (2011) Adsorption of Cu(II) by biochars generated from three crop straws. *Chem Eng J* 172:828–834. doi:10.1016/j.cej.2011.06.069
- Tripathi M, Sahu JN, Ganesan P (2016) Effect of process parameters on production of biochar from biomass waste through pyrolysis: a review. *Renew Sustain Energy Rev* 55:467–481. doi:10.1016/j.rser.2015.10.122
- Turrado Fernández S, Paredes Sánchez JP, Gutiérrez Trashorras AJ (2015) Analysis of forest residual biomass potential for bioenergy production in Spain. *Clean Technol Environ Policy*. doi:10.1007/s10098-015-1008-8
- Ubando AT, Culaba AB, Aviso KB et al (2014) Fuzzy mixed-integer linear programming model for optimizing a multi-functional bioenergy system with biochar production for negative carbon emissions. *Clean Technol Environ Policy* 16:1537–1549. doi:10.1007/s10098-014-0721-z
- Uchimiya M, Klasson KT, Wartelle LH, Lima IM (2011a) Influence of soil properties on heavy metal sequestration by biochar amendment: 1. Copper sorption isotherms and the release of cations. *Chemosphere* 82:1431–1437. doi:10.1016/j.chemosphere.2010.11.050
- Uchimiya M, Wartelle LH, Klasson KT et al (2011b) Influence of pyrolysis temperature on biochar property and function as a heavy metal sorbent in soil. *J Agric Food Chem* 59:2501–2510. doi:10.1021/jf104206c
- Vithanage M, Rajapaksha AU, Ahmad M et al (2015) Mechanisms of antimony adsorption onto soybean stover-derived biochar in aqueous solutions. *J Environ Manag* 151:443–449. doi:10.1016/j.jenvman.2014.11.005
- Vochozka M, Maroušková A, Váchal J, Straková J (2016a) Biochar pricing hampers biochar farming. *Clean Technol Environ Policy*. doi:10.1007/s10098-016-1113-3
- Vochozka M, Maroušková A, Váchal J, Straková J (2016b) Reengineering the paper mill waste management. *Clean Technol Environ Policy* 18:323–329. doi:10.1007/s10098-015-1012-z
- Wang S, Gao B, Zimmerman AR et al (2014) Removal of arsenic by magnetic biochar prepared from pinewood and natural hematite. *Bioresour Technol* 175C:391–395. doi:10.1016/j.biortech.2014.10.104
- Wang S, Gao B, Li Y et al (2015a) Manganese oxide-modified biochars: preparation, characterization, and sorption of arsenate and lead. *Bioresour Technol* 181:13–17. doi:10.1016/j.biortech.2015.01.044
- Wang S, Gao B, Zimmerman AR et al (2015b) Physicochemical and sorptive properties of biochars derived from woody and herbaceous biomass. *Chemosphere* 134:257–262. doi:10.1016/j.chemosphere.2015.04.062
- Wen B, Zhang J, Zhang S et al (2007) Phenanthrene sorption to soil humic acid and different humin fractions. *Environ Sci Technol* 41:3165–3171. doi:10.1021/es062262s
- Wiedemeier DB, Abiven S, Hockaday WC et al (2015) Aromaticity and degree of aromatic condensation of char. *Org Geochem* 78:135–143. doi:10.1016/j.orggeochem.2014.10.002
- Wu H, Gao G, Zhou X, Zhang Y, Guo S (2012) Control on the formation of Fe₃O₄ nanoparticles on chemically reduced graphene oxide surfaces. *CrystEngComm* 14:499–504. doi:10.1039/C1CE05724C
- Xiu S, Shahbazi A, Wang L, Wallace CW (2010) Supercritical ethanol liquefaction of swine manure for bio-oils production Department of Natural Resource and Environmental Design, Biological Engineering Program, North Caroli. *Am J Eng Appl Sci* 3:494–500
- Yang JE, Skogley EO, Ahmad M et al (2013) Carbonaceous resin capsule for vapor-phase monitoring of volatile hydrocarbons in soil: partitioning and kinetic model verification. *Environ Geochem Health* 35:715–725. doi:10.1007/s10653-013-9529-8
- Yao Y, Gao B, Inyang M et al (2011a) Removal of phosphate from aqueous solution by biochar derived from anaerobically digested sugar beet tailings. *J Hazard Mater* 190:501–507. doi:10.1016/j.jhazmat.2011.03.083
- Yao Y, Gao B, Inyang M et al (2011b) Biochar derived from anaerobically digested sugar beet tailings: characterization and phosphate removal potential. *Bioresour Technol* 102:6273–6278. doi:10.1016/j.biortech.2011.03.006
- Yao Y, Gao B, Chen J et al (2013) Engineered carbon (biochar) prepared by direct pyrolysis of Mg-accumulated tomato tissues: characterization and phosphate removal potential. *Bioresour Technol* 138:8–13
- Yao Y, Gao B, Fang J et al (2014) Characterization and environmental applications of clay–biochar composites. *Chem Eng J* 242:136–143. doi:10.1016/j.cej.2013.12.062
- Yargicoglu EN, Sadasivam BY, Reddy KR, Spokas K (2015) Physical and chemical characterization of waste wood derived biochars. *Waste Manag* 36:256–268. doi:10.1016/j.wasman.2014.10.029
- Zhang M, Gao B (2013) Removal of arsenic, methylene blue, and phosphate by biochar/AlOOH nanocomposite. *Chem Eng J* 226:286–292. doi:10.1016/j.cej.2013.04.077
- Zhang M, Gao B, Yao Y et al (2012a) Synthesis of porous MgO–biochar nanocomposites for removal of phosphate and nitrate from aqueous solutions. *Chem Eng J* 210:26–32. doi:10.1016/j.cej.2012.08.052
- Zhang M, Gao B, Yao Y et al (2012b) Synthesis, characterization, and environmental implications of graphene-coated biochar. *Sci Total Environ* 435–436:567–572. doi:10.1016/j.scitotenv.2012.07.038
- Zhang M, Gao B, Vamoosfaderani S et al (2013a) Preparation and characterization of a novel magnetic biochar for arsenic removal. *Bioresour Technol* 130:457–462. doi:10.1016/j.biortech.2012.11.132
- Zhang M, Gao B, Yao Y, Inyang M (2013b) Phosphate removal ability of biochar/MgAl-LDH ultra-fine composites prepared by liquid-phase deposition. *Chemosphere* 92:1042–1047. doi:10.1016/j.chemosphere.2013.02.050
- Zhang J, Zhong Z, Zhang B et al (2016) Prediction of kinetic parameters of biomass pyrolysis based on the optimal mixture design method. *Clean Technol Environ Policy*. doi:10.1007/s10098-016-1137-8
- Zhao MY, Enders A, Lehmann J (2014) Short- and long-term flammability of biochars. *Biomass Bioenergy* 69:183–191. doi:10.1016/j.biombioe.2014.07.017
- Zhou Y, Gao B, Zimmerman AR et al (2014a) Biochar-supported zerovalent iron for removal of various contaminants from aqueous solutions. *Bioresour Technol* 152:538–542. doi:10.1016/j.biortech.2013.11.021
- Zhou Y, Gao B, Zimmerman AR, Cao X (2014b) Biochar-supported zerovalent iron reclaims silver from aqueous solution to form antimicrobial nanocomposite. *Chemosphere* 117:801–805. doi:10.1016/j.chemosphere.2014.10.057
- Zimmerman AR (2010) Abiotic and microbial oxidation of laboratory-produced black carbon (biochar). *Environ Sci Technol* 44:1295–1301. doi:10.1021/es903140c